Stratified Flow in a Wind Tunnel Environment

Marcio Cataldi
Mechanical Engineering Program (PEM/COPPE/UFRJ), Federal University of Rio de Janeiro, C.P. 68503, 21945-970 - Rio de Janeiro - Brazil.
mcataldi at serv.com.ufrj.br

Juliana B. R. Loureiro
Mechanical Engineering Department (DEM/EE/UFRJ), Federal University of Rio de Janeiro, C.P. 68503, 21945-970 - Rio de Janeiro - Brazil.
jbrloureiro at serv.com.ufrj.br

Daniel A. Rodrigues
Mechanical Engineering Department (DEM/EE/UFRJ), Federal University of Rio de Janeiro, C.P. 68503, 21945-970 - Rio de Janeiro - Brazil.
darodrigues at serv.com.ufrj.br

Atila P. Silva Freire
Mechanical Engineering Program (PEM/COPPE/UFRJ), Federal University of Rio de Janeiro, C.P. 68503, 21945-970 - Rio de Janeiro - Brazil.
atila at serv.com.ufrj.br

Abstract. *The present work will show how stratified boundary layer flows can be achieved in a wind tunnel environment. The main objective is to produce boundary layers with different states of development that can simulate the structure present in the atmospheric boundary layer. The work analyzes the dynamic and thermal characteristics of different types of artificially generated turbulent boundary layers. The thermal boundary layer is obtained by two methods: wall surface heating and main flow heating. The wall surface heating, made through electrical resistances, can furnish an increase in wall temperature of up to 100 ^oC above the ambient temperature and can be applied over a 6000 mm long surface with a controlled variation of 2 ^oC. The main flow heating is obtained by forcing the flow pass through a set of copper resistances whose elements can the heated individually. The main flow can be heated up to 50 ^oC. The whole system can then be used to produce, unstable, neutral and stable boundary layers. The parameters of the thermal boundary layer are qualified through: growth, structure, equilibrium, turbulent transport of heat and energy spectrum. The paper describes in detail the experimental arrangement, including the geometry of the wind tunnel and of the instrumentation. Thus, an investigation of the most suitable hot-wire/cold-wire calibration laws for measurements in stratified, low Reynolds number flows is presented. The results are shown in the form of tables, equations and calibration curves for temperature and velocity data. An uncertainty analysis of the results is also given. Some measurements of simulated stratified atmospheric conditions are presented so as to illustrate the potential of hot wire anemometry for extracting information on various aspects of the turbulent motion.*

Keywords: *Stratification, atmospheric boundary layer, wind tunnel.*

1. Introduction

The direct observation of atmospheric flows is a very difficult and costly affair. In fact, to observe natural flows, the common practice is to use instruments attached to fixed towers or fitted to aircrafts, balloons or kites. In all cases the difficulties are many and the costs high. An alternative approach is to resort to laboratory observation. The advantages of a controlled laboratorial study are many. However, extreme care must be taken to ensure that data obtained in wind tunnels show good similarity with corresponding atmospheric data. Since the number of parameters that influence the atmospheric boundary layer is large this is a very difficult task. Typical parameters are the cycle of solar heating of the ground, mesoscale phenomena and ground orography.

Because the temperature in the atmosphere changes abruptly with height air parcels displaced vertically will experience net buoyancy forces resulting in persistent stratified flow states. Thus, if reliable numerical weather prediction and circulation models are to be proposed, the dynamics of stratified flows must be well understood. Of particular interest in this subject is the account of small scale phenomena on the flow features.

The purpose of this article is to present the results of a series of stratified wind tunnel experiments carried out at PEM/COPPE/UFRJ. The experiments aimed at producing stable, neutral and unstable flows in a short wind tunnel. To generate boundary layers that satisfied the requirements for geometric, dynamic and thermal similarity with the atmospheric boundary layer several special measures were taken. Data validation was made by comparison of results obtained in the present facilities with data taken from other laboratories and the field.

The present work is part of a larger effort whose aims are: i) to investigate methods of simulating stable, neutral and unstable boundary layers in a wind tunnel, ii) to study the effects of rough surfaces on stratified boundary layers, and iii) to study the effects of orography on stratified boundary layers.

The paper shows how the boundary layer that is formed over the floor of the wind tunnel is controlled by heating the floor and the incoming air through electrical resistances. The resistances can furnish an increase in floor temperature of up to 100^oC above ambient temperature and can be applied over a 6000 mm long surface with a controlled variation of $\pm 5^o C$. The incoming air is heated by forcing the flow through a set of 10 electrical heating elements which can be operated individually. The system can then be used to produce, unstable, neutral and stable boundary layers. Despite the 6000 mm heating length, only 2000 mm will be used in this work; that is because we were particularly interested in producing stratified flows over a short length.

To create a thick boundary layer in the wind tunnel we resort to the method developed by Barbosa et al.(2000). In their work, these authors show how a combination of spires and bars can be used to generate boundary layers as thick as 28 cm over lengths as short as 5 meters. The experimental assessment of the thickening device was carried out considering the integral properties of the flow, skin-friction, mean velocity profiles in inner and outer coordinates and turbulence.

An extra word seems now in order. Normally, wind tunnels are asked to run at high velocities, as most of the experimental facilities around these days were built aimed at aeronautical applications. Instrumentation, therefore, including hardware and software, were normally developed for high speed flows. Wind tunnels for environmental applications, however, run at low speeds. As such, particular techniques have to be developed to handle this type of flow. In addition, environmental applications require almost as a role the analysis of flows subject to abrupt changes in temperature.

Investigations of the velocity field on turbulent, unheated, steady flows concerning hot wire anemometry have already received considerable attention. However, only a handful studies are available for unsteady, heated flows. Most of cold-wire anemometry literature is restricted to situations where only a slight compensation for ambient temperature deviations is need to correct the hot-wire signal. Bremhost(1985) reviewed difficulties and methods associated with correct velocity measurements in heated flows using hot-wire anemometers and proposed a method for automatic compensation to give a corrected, instantaneous velocity signal by use of a hot and cold-wire anemometers simultaneously. The method was limited to flows with a spectral content below the corner frequency response of the cold wire.

Nevertheless, as said before, in atmospheric flows stratification conditions exert a great influence on the velocity field, requiring the simultaneous measurement of instantaneous velocity and temperature for a correct characterization of any phenomena under study. Hence, in this work we will present an extension of resistance wires for the investigation on the influence of the temperature field in the properties of boundary layers, so as to obtain a better understanding of the mixing processes involved in such problems.

In general, one of the most important aspects of thermal anemometry is the accurate interpretation of the anemometer signal. The main purpose of any sensor calibration is to determine, as accurately as possible, the relationship between the anemometer output voltage and the physical property under consideration, in this case velocity or temperature. However, the direct output from all practical calibration procedures is raw calibration data which will contain measurements uncertainties. An additional complication is that the true calibration curve of the probe is not known, and furthermore it depends on particular characteristics of each experiment.

In this work we will then investigate an appropriate method of curve fitting the data, for measurements on specific conditions of low velocity and temperature gradients. The work also intends to minimise any experimental error if a good accuracy is to be obtained. Those aspects were considered in both the velocity and temperature measurements, with the main purpose being to compare several curve fitting methods on a commom basis, by using the same input data, and to identify both accuracy and suitability for implementation on a microcomputer. Measurements of stratified boundary layers illustrates the accuracy of the method used. A discussion of uncertainty analysis is also made.

Before moving to the main part of the article we will first present a short revision of the conditions in which boundary layer similarity is achieved.

2. Similarity Conditions

The general requirements for similarity of flows are dictated by the equations of motion – conservation of mass, momentum and energy. To simulate the atmospheric boundary layer in a wind tunnel the large number of dimensionless groups that would have to be matched to assure exact similarity seems to render the problem impossible to solve since, in principle, all conditions would have to be satisfied simultaneously by the model and some are incompatible or even conflicting. Thus, only approximate similarity can be achieved in a laboratory experiment; it results that small scale experiments must be designed to represent accurately the characteristics of motion which are of most importance for the desired application.

Following the procedure of Cermak(1971) we take as the basic physical model a boundary layer developed over the floor of a wind tunnel test section in which vertical temperature gradients are controlled by heating. The effects of radiation heat transfer and phase changes of water in the atmosphere will not be accounted for in the present analysis. Also, extreme meteorological events which give rise to local singular motions are not contemplated here.

The requirements for geometric, dynamic and thermal similarity can be obtained by direct inspection of the equations of motion. The equation of continuity remains invariant when transformed to dimensionless form provided a same characteristic length is taken for the vertical and horizontal directions.

$$\frac{\partial \rho}{\partial t} + \frac{\partial \rho U_i}{\partial x_i} = 0. \tag{1}$$

The momentum equation can be cast as

$$\frac{\partial U_i}{\partial t} + U_j \frac{\partial U_i}{\partial x_j} + \frac{1}{R_o} 2\epsilon_{ijk}\Omega_j U_k = -\frac{\partial P}{\partial x_i} - R_i(\Delta T) g \delta_{i3} + \frac{1}{R_e}\frac{\partial^2 U_i}{\partial x_k \partial x_k} + \frac{\partial}{\partial x_j}\langle -u_i' u_j' \rangle, \tag{2}$$

by scaling all variables in relation to the reference quantities L_0, U_0, Ω_0, ρ_0, ΔT_0 and g_0. Equation 2 is the time averaged Navier-Stokes equation where all variables represent a mean value. The fluctuating variables are indicated by a dash and the brackets $\langle\ \rangle$ indicate an average operation. U_i stands for the velocity component in the x_i direction, p for the pressure, g for the gravitational acceleration, ΔT for the temperature deviation, ν for the kinematic viscosity, Ω for earth's angular velocity and ϵ_{ijk} for the permutation tensor.

The effects of temperature stratification on the velocity field have been accounted for by Boussinesq approximation; this limits equation 2 to situations where $\Delta T << T_0$ and implies that p is the departure of the mean pressure from the hydrostatic pressure for an atmosphere of density ρ_0.

Equation 2 leads to the conclusion that complete dynamic similarity depends on the following dimensionless groups:

Rossby number; $R_o = U_0/L_0\Omega_0$,
Reynolds number; $R_e = U_0L_0/\nu_0$,
Richardson number; $R_i = [(\Delta T_0)T_0](L_0/U_0^2)g_0$.

When no rotation is imposed on the wind tunnel about a vertical axis, the Rossby number for the wind tunnel will be smaller than that for the atmosphere by a factor of approximately 10^{-3} (the length scale). This is a serious limitation to laboratory simulation of atmospheric flows for we know that at geostrophic heights, when the pressure forces and the Coriolis forces reach equilibrium, wind direction varies by an angle of 10^o to 30^o from ground level. Some author have removed this limitation by introduction of a cross flow through porous walls of a stationary wind tunnel or by use of a large rotating flow chamber (Cermak(1971)); this has incurred in very high costs and great operational difficulties. Rossby number similarity will, hence, be excluded from the present analysis. This limits our representation of the atmospheric boundary layer to the first 150 meters from ground level. This portion of the atmospheric boundary layer is referred to in literature as the atmospheric surface layer.

The Reynolds number for the wind tunnel will also be 10^{-3} smaller than that for the atmosphere. Reynolds number similarity is therefore not achievable. This fact, however, does not add much problem to our attempt at modelling the atmosphere for we know that for flows over rough surfaces the near wall flow becomes independent of viscosity, being a function of the roughness scale. Since all natural surfaces are rough, the flow structure related to momentum transfer will be equal provided the roughness lengths are appropriately scaled down.

The bulk Richardson number that is typical of the atmosphere, -1 $< R_i <$ 1, can be obtained in a wind tunnel.

Thermal similarity is studied through the energy equation.

$$\frac{\partial T}{\partial t} + U_i\frac{\partial T}{\partial x_i} = \frac{1}{R_eP_r}\frac{\partial^2 T}{\partial x_k \partial x_k} + \frac{\partial}{\partial x_i}\langle -\theta_i' u_j' \rangle + \frac{E_c}{R_e}\Phi. \tag{3}$$

Equation 3 adds two dimensionless groups to our problem:

Prandtl number; $P_r = \nu_0/(k_0/\rho_0 C_{p0})$,
Eckert number; $E_c = U_0^2/C_{p0}(\Delta T)_0$.

If air is used as the working fluid in the wind tunnel, Prandtl number similarity is immediately achieved. The influence of Eckert number on similarity considerations is not relevant until the flow approaches the speed of sound, this requirement is therefore relaxed.

In addition to equality of the dimensionless groups, requirements assuring that the boundary conditions and the approach-flow characteristics are similar for the wind tunnel and the atmosphere must be observed.

Similarity of surface conditions is characterized by the following factors:

1. Surface roughness,
2. topographic relief,
3. surface temperature distribution.

The approach-flow is characterized by:

1. Upstream distribution of mean and turbulent velocities,
2. upstream distribution of mean and turbulent temperatures,
3. longitudinal pressure gradient.

3. Instrumentation

In all experiments, simultaneous measurements of stream-wise velocity and fluctuating temperature were obtained by using thermal anemometry. The measurements accounted for any large temperature variation in interpreting the sensor response. To perform the measurements a temperature-compensated Dantec probe, model 55P76, was used. This probe consists of two sensor elements: a hot-wire and a resistance-wire, usually called cold-wire, situaded 2 mm below and 5 mm downstream of the former. Both sensors are Pt-plated tungsten wires, 5 μm in diameter, overall length of 3mm and sensitive wire length of 1,25 mm. They are copper and gold plated at the ends to approximately 30 μm. They were connected respectively to a constant temperature bridge, Dantec 55M10 and to a constant current brigde, Dantec 56C20.

For the measurement of both velocity components, u and v, an X hot-wire Dantec probe, model 55P51, was used with the sensors set in a plane parallel to the probe axis.

Reference measurements for velocity was obtained from a Pitot tube connected to an inclined manometer; temperature reference data was obtained from previously calibrated microthermocouples.

3.1. Calibration Characterization

Among the several possible methods that can be devised to characterize the velocity and temperature dependence of thermal anemometers signals, it is possible two classify them in three main categories (Freymuth, 1970):

1. The linear correction method where the heat transfer from the probe is assumed to be proportional to a product of the temperature difference $T_w - T_a$ and a function of the velocity, where T_w is the temperature of the heated wire and T_a is the ambient temperature. The output voltage, E, of a constant temperature hot-wire anemometer can hence be represented by:

$$E^2 = f(U)(T_w - T_a). \tag{4}$$

2. The convective heat transfer is expressed in a non-dimensional form involving a relationship between the Nusselt number, Nu, the Reynolds number, Re, and the Prandtl number, Pr.
3. Direct calibration of the variation in the anemometer output voltage, E, with the velocity, U, and the fluid temperature, T_a, for a given hot resistance setting, R_w.

The third method is the most complex to implement but it is also the most accurate, and will be adopted in this work. The calibration data obtained by this method can reveal to what an extent the other methods can be used to evaluate the temperature and velocity sensitivity of a hot-wire probe operated in the CT mode.

3.2. Temperature Calibration for the Cold-Wires

Fluid temperature measurements are often performed with a hot-wire sensor operated in the constant-current mode at very low overheat ratio, in order to minimise Joule heating. Ideally, the wire sensor behaves like a resistance thermometer.

Temperature measurements with resistance wires require both low drift, low noise constant current anemometers and high quality amplifiers. If the resistance wire is heated by a current $I = 0.15mA$, then the "hot" resistance R_w will only deviate from R_a by $(R_w - R_a)/R_a \simeq 0.0004$, and the corresponding temperature difference $(T_w - T_a)$ will be less than $0.1\ ^oC$.

Thus, a common practice is to consider $R_w = R_a$, with

$$R_a = R_0\,[1 + \alpha_0(T_a - T_o)]. \tag{5}$$

For practical applications, it is recommended that a temperature calibration of the resistance-wire is used to determine the calibration constants in the relationship

$$R_a = A + B\,T_a. \tag{6}$$

3.3. Temperature and Velocity Calibration for Hot-Wires

The most accurate way of establishing the velocity and temperature sensitivity of a constant temperature hot-wire probe, operated at a fixed hot resistance, R_w, is to measure the anemometer output voltage, E_w, as a function of the velocity, U, and fluid temperature, T_a. This type of calibration is often carried out by performing a velocity calibration at a number of different fluid temperatures.

The functional form of the calibration data may be evaluated as

$$E = F(U, T_a)_{T_w = const}, \tag{7}$$

but, more commonly, the calibration data have been interpreted in the form

$$E = F(U, T_a - T_w)_{T_w = const}. \tag{8}$$

To evaluate T_w it is necessary to measure the hot resistance, R_w, and this requires a knowledge of the probe and cable resistance. The mean wire temperature, T_w, corresponding to R_w is normally determined by the equation:

$$R_w = R_0\,[1 + \alpha_0(T_w - T_0)], \tag{9}$$

where the temperature coefficient of resistance, α_0, is a property that is usually given by the manufacturer of the probe.

For single normal probes, in this case the hot-wire probe, the classical convective heat transfer law, King´s law, can be written as

$$E^2 = A + BU^n, \tag{10}$$

where A, B and n are empirical constants.

Equation 10 is a very good approximation to the velocity calibration data, obtained at a constant value of T_a, provided the calibration constants are determined by a least-squares curve fit. This procedure has been applied by other authors to their velocity calibration data using the wire voltage relationship

$$\frac{E_w^2}{R_w\,(R_w - R_a)} = A + BU^n. \tag{11}$$

This curve-fitting procedure gave the most accurate results, but A, B, and n were found to be functions of T_a. When a constant value of $n(= 0.45)$ was selected, A and B also became constants, and the increase in the uncertainty is insignificant for most hot wire anemometry aplications.

A similar approach was adopted by Lemieux and Oosthuizen(1984). They expressed their calibration relationship in the form

$$E^2 = A^* + B^* U^n, \tag{12}$$

and for each value of T_a they determined the values of A^*, B^* and n by a least squares curve fitting procedure. In their subsequent signal analysis the optimum value for n was selected as being the average value from their four calibration curves. The corresponding calibration coefficients A^* and B^* were found to vary linearly with T_a:

$$A^* = A_1 + A_2 T_a, \tag{13}$$

$$B^* = B_1 + B_2 T_a. \tag{14}$$

A linear variation of E^2 with T_a has also been reported by other authors. In conclusion, most experimental investigations of this type, covering small or moderate variations in T_a, have demostrated that the output signal from a hot-wire probe operated in the constant temperature mode is directly proportional to a product of the temperature difference $(T_w - T_a)$ and a function of the velocity.

3.4. X Hot-wire Calibration

Two-component velocity measurements are commonly performed with a probe with two wires placed in an X-configuration. For signal analysis purpose, one normally assumes that the two wires are contained in the same plane. However, for practical purposes the two wires cannot be placed too close together or else the thermal wake from one wire will affect the output from the other wire. Jerome et al.(1971) have shown that if a wire spacing of about 1 mm is used, then, the hot-wake effect is negligible. Despite some operating difficulties such as prong-wake problems and aerodynamic disturbances effects, X-probes have become very popular over the years.

For calibration and evaluation purposes the standard procedure is to consider that velocity component perpendicular to the X-probe is small compared to the velocities in the two in-plane components ,U and V, so that the response equations for the two-wires can be expressed as

$$E_1 = F_1(U,V) = F_3(\tilde{V},\theta,\alpha), \tag{15}$$

$$E_2 = F_2(U,V) = F_4(\tilde{V},-\theta,\alpha). \tag{16}$$

where $\tilde{V}$ denotes the magnitude of the flow vector, θ the flow angle and α the yaw angle of the wires.

A simplified calibration procedure and signal analysis can be developed by introducing the effective-velocity concept whereby we consider

$$\begin{aligned} V_e &= \tilde{V} f(\alpha) = \tilde{V}(\cos^2\alpha + k^2 \sin^2\alpha)^{1/2}, & (17)\\ &= (U_N^2 + k^2 U_T^2)^{1/2}. & (18) \end{aligned}$$

$$k = \frac{1}{\sin\alpha}\big[\big(\frac{E^2(\alpha) - A}{E^2(0) - A}\big)^{1/2} - \cos^2\alpha\big]^{1/2}. \tag{19}$$

Then, the response equation for the two wires can be written as

$$E_1^2 = A + BV_{e1}^n, \tag{20}$$

$$E_2^2 = A + BV_{e2}^n, \tag{21}$$

Thus for the complete velocity and flow-angle range the X-probe calibration relationship can be expressed as

$$E^2 = A(\theta) + B(\theta) V_e^{n(\theta)}. \tag{22}$$

The so called V_e-calibration method consider each wire in the X-probe independent, so that a standard calibration for a single inclined probe is used. The result is that a simple expression for V_e can be cast as

$$V_e = f(\alpha)\,[U - g(\alpha)v], \tag{23}$$

where

$$f(\alpha) = (\cos^2\alpha + k^2\sin^2\alpha)^{1/2}, \tag{24}$$

$$g(\alpha) = \frac{(1-k^2)\cos^2}{(\cos^2\alpha + k^2\sin^2\alpha)}\tan\alpha. \tag{25}$$

The values of U and V can then be obtained by the modified sum-and-difference procedure, which yields

$$U = \frac{[V_{e1}/f_1(\alpha_1)]g_2(\alpha_2) + [V_{e2}/f_2(\alpha_2)]g_1(\alpha_1)}{g_1(\alpha_1) + g_2(\alpha_2)}, \tag{26}$$

$$V = \frac{[V_{e2}/f_2(\alpha_2)] + [V_{e1}/f_1(\alpha_1)]}{g_1(\alpha_1) + g_2(\alpha_2)}, \tag{27}$$

For flows subject to temperature variations, parameters A and B must be considered dependent not only on θ but also on T.

3.5. Calibration Results

In the following we will describe the calibration procedure for both the hot-wire and the cold-wire; emphasis will be placed on the cold-wire procedure.

The calibration was performed in the low-turbulence wind tunnel sited in the Laboratory of Turbulence Mechanics of PEM/COPPE/UFRJ.

- Circuit: open.
- Test section: 0.30 m high, 0.30 m wide and 2 m long.
- Wind speed: continuously variable from 0.5 to 16 m/s.
- Longitudinal pressure gradient: adjustable to zero by means of an adjustable ceiling.
- Turbulence intensity: below 0.2%.
- Incoming flow temperature: variable from 20 to 35^oC.
- Number of resistances used to heat the incoming air: 4.
- Resistances capacity: 7 KW.

A general view of the low-turbulence wind tunnel is shown in Figure 1.

Figure 1. General view of the low-turbulence wind tunnel and the heating elements.

Table 1: Typical calibration range for a cold-wire anemometer.

Author	Velocity Range (mm)	Temperature Range ^oC
Pessoni and Chao(1974)	6 to 0	22 to 60
Koppius and Trines(1976)	0.5 to 5	10 to 80
Fiedler(1978)	2 to 20	21 to 50
Dekeyeser and Launder(1983)	7.6 to 15.4	25 to 35
Lemieux and Oosthuizer(184)	0.5 to 4	25 to 55
Bremhorst(1985)	1.5 to 35	20 to 80
COPPE/UFRJ	0.5 to 3.0	20 to 35

For the present measurements, a DANTEC 55M01 main unit together with a 55M20 constant current bridge was used. The boundary layer probe was of the type 55P76. A Pitot tube, an electronic manometer, and a computer controlled traverse gear were also used. In getting the data, 10,000 samples were considered. The reference mean temperature profiles were obtained through a chromel-constantan micro-thermocouple mounted on the same traverse gear system used for the hot-wire probe. An uncertainty analysis of the data was performed according to the procedure described in Kline[20]. Typically the uncertainty associated with the velocity and temperature measurements were: $U = 0.0391\ m/s$ precision, 0 bias (P=0.95); $T = 0.2\ ^oC$ precision, 0 bias (P=0.99).

To obtain accurate measurements, the mean and fluctuating components of the analogical signal given by the anemometer were treated separately. Two output channels of the anemometer were used. The mean velocity profiles were calculated directly from the untreated signal of channel one. The signal given by channel two was 1 Hz high-pass filtered leaving, therefore, only the fluctuating velocity. The latter signal was then amplified with a gain controlled between 1 and 500 and shifted by an offset so as to adjust the amplitude of the signal to the range of the A/N converter.

The typical calibration range for a cold-wire probe is shown in Table 1.

The dependence of the hot-wire voltages, E_w, on the air velocity, U, for different ambient temperatures is shown in Figure 2.

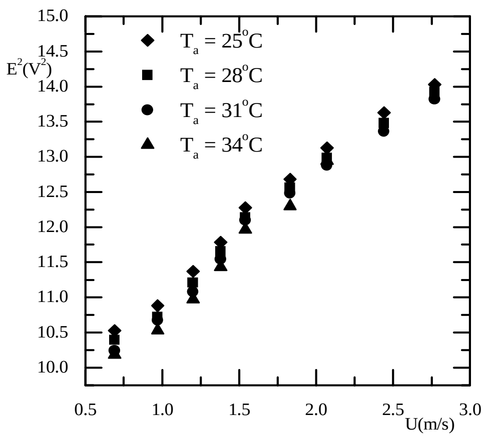

Figure 2. The dependence of hot-wire voltage on the air velocity for different ambient temperatures.

The calibration coefficients $A*$ and $B*$ corresponding to the curves in Figure 2 were found to vary linearly with T_a. A linear variation of E^2 with T_a as been observed by Fulachier(1978), by Champagne(1978) and by Dekeyser and Launder(1983).

The present data were obtained with a 5 μm diameter tungsten wire with an overheat ratio of 1.8; this corresponds to a temperature difference T_W - T_a of about 220 ^oC.

In conclusion, and after other authors, we have found that the signal from a hot-wire probe operated in the constant temperature mode is directly proportional to a product of the temperature difference and a function of the velocity.

Figure 3 shows the variation of the calibration parameters $A*$ and $B*$ with the fluid temperature.

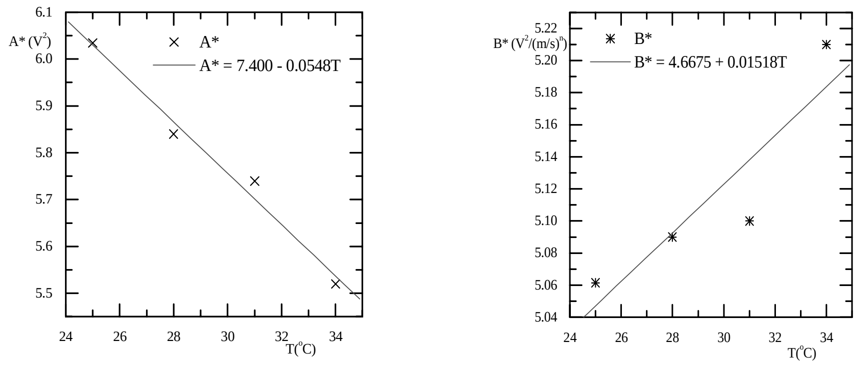

Figure 3. Variation of the calibration parameters $A*$ and $B*$ with the fluid temperature.

The X-probe was calibrated through the V_e-calibration method whereby each wire in the probe is calibrated independently, and the calibration procedure for the inclined probe is used. The calibration of both wires was performed simultaneously so that a least-square curve-fitting could be used to find A_1, B_1, A_2, B_2. The X-probe calibration map is shown Figure in 4.

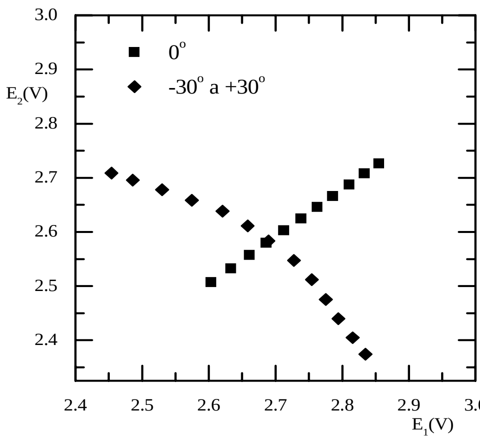

Figure 4. Calibration map for the X-wire probe.

4. Wind Tunnel Design

The size of the wind tunnel test section will determine the model length scale ratio (LSR). Many wind tunnels are designed to represent the first 500 m of the atmosphere. For these, a scale ratio of 1:500 is used so that one meter thick boundary layers will have to be produced in the laboratory. Boundary layers with this thickness require very long test sections to be achieved resulting in large experimental facilities. Meteorological wind tunnels can have a working cross section as large as 7x12 meters with a total section length of 40 meters (Monasch University). However, many other tunnels present much short working cross sections varying from 0.5x0.5 m to 3x4 m. Design recommendations have been advanced by several authors, Cermak(1971, 1975, 1981), Poreh et al.(1991), Meroney and Melbourne(1992), Grainger and Meroney(1994), Ohya et al.(1994) and Fedorovich et al.(1996). All authors agree that ideally an atmospheric wind tunnel should have a working section longer than 10 meters. Indeed, Cermak(1975) has shown that only after 10 meters from the test section entrance the turbulent boundary layer becomes fully developed. This is in agreement with the findings of other authors. Furthermore, Poreh et al.(1991) have shown that the minimum desired wind tunnel dimension for diffusion experiments is 10 meters.

The general features of typical atmospheric wind tunnels are shown in Table 2. To construct this table, data was taken from the following facilities: Cornell University, Ithaca, USA, Yoon(1990); Colorado State University, Fluid Dynamics and Diffusion Laboratory, USA, Cermak(1975); Ecole Centrale de Lyon, Ecully, France, Reynolds(1978); Institut für Hydrologie und Wasserwirtschaft, Karlsruhe, Alemanha, Rau(1991); Research Institute for Applied Mechanics, Kyushu University, Kasuga, Japan, Ohya(1996); Dept.Mechanical Engineering, Monash University, Australia, Grainger(1994); Mitsubishi Heavy Industries, Nagasaki, Japan, Ohba(1990); National Institute for Environmental Studies, Ibaraki, Japan, Ogawa(1981).

Table 2: Atmospheric wind tunnel features.

	C. S.	L.	U	dT/dz	δ
Cornell	0.91x0.91	9.14	2.8-4.2	55	
Colorado	1.8x1.8	24	0.1 to 30	114	1.4
ECL	1.2x1	10	1 to 20		0.4
Karlsruhe	1.5x1.5	10	0.5-8	120	0.75
Kyushu	1.5x1.2	13.5	0.2-2	125	
Monash	10x5	40	0.5		0.3
MHI	2.5x1	10	0.4-1.5		
NIES	3x2.4	24	0.2-10	25	1

Table 3: Wind tunnel instrumentation.

	HWA	LDA	CWT	Th	MWT	P_W
Cornell	Yes		Yes			
Colorado	Yes	Yes	Yes	Yes	205	
ECL	Yes		Yes		100	
Karlsruhe		Yes	Yes	Yes		32
Kyushu				Yes	4-80	50
Monash	Yes		Yes			9
MHI	Yes	Yes	Yes	Yes	0-100	7
NIES	Yes		Yes	Yes	7-112	

The instrumentation used in these tunnels is reviewed in Table 3.

The data in Tables 2 and 3 give us some criteria as to what should be the operating range of an atmospheric wind tunnel. At this point we recognize that by using vortex generators and roughness elements, a large range of integral scales can be introduced into the boundary layer. In fact, a previous study by Barbosa et al.(2000) showed how a simple combination of cylindrical rods and rectangular bars can be used to produce artificial boundary layers with thicknesses up to 27 cm in a 5 m short wind tunnel test section. The experimental assessment of the generators was carried out by considering the integral properties of the flow, skin-friction, mean velocity profiles in inner and outer coordinates and turbulence.

Because of the very high cost involved in designing, constructing and operating a large atmospheric wind tunnel, we have decided at COPPE/UFRJ to construct a small pilot tunnel. The tunnel, if possible, should be capable of reproducing stable, neutral and unstable flows.

After careful consideration, a wind tunnel with the following characteristics was constructed:

- Circuit: open.
- Test section: 0.67 m high, 0.67 m wide and 10 m long.
- Wind speed: continuously variable from 0.5 to 3 m/s.
- Longitudinal pressure gradient: adjustable to zero by means of an adjustable ceiling.
- Turbulence intensity: 2%.
- Surface heating capacity: 5 KW m^2.
- Length of wall heating section: 6 m.
- Wall temperature: variable from 21 to 100^oC.
- Number of resistances used to heat the incoming air: 10.
- Resistances capacity: 2 KW.
- Vortex generators: rods with 1/8" diameter and 16 mm length spaced by 10 mm. One or two trailing transversal trips were also used.

A general view of the wind tunnel can be seen in Figure 5 together with a drawing illustrating the positioning of the heating elements.

Table 4: Atmospheric boundary layer characteristics (Driffield Power Station, Australia).

Inversion Height, zi:	1000 m
Mean Velocity:	4 m/s
Mean Temperature:	20 ^{o}C
Heat Flux:	400 W/m^2

Table 5: Global flow parameters.

	Stable		Neutral		Convective	
	ABL	WT	ABL	WT	ABL	WT
G	5.09	6.77	7.45	7.71	6.27	8.98
u_τ	0.09	0.06	0.08	0.07	0.10	0.12
δ	0.05	0.11	0.05	0.14	0.05	0.11
δ_2	0.004	0.011	0.007	0.018	0.005	0.013
n	0.2	0.21	0.2	0.22	0.25	0.35


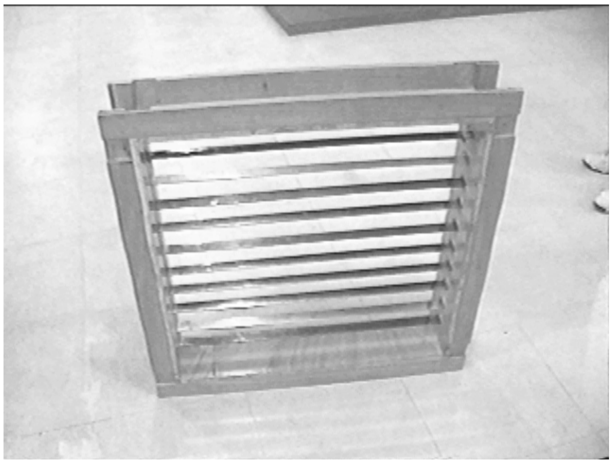

Figure 5. General view of wind tunnel and the heating elements.

5. Wind Tunnel Performance

The results provided the wind tunnel constructed at COPPE/UFRJ will be compared here with some real flow data and data of other authors. Typical atmospheric conditions are shown in Table 4.

The global flow parameters are shown in Table 5 where G stands for the Clauser factor, u_τ for the skin-friction velocity, δ for the boundary layer thickness, δ_2 for the momentum thickness and n for the exponent in the power law.

We clearly see that both the naturally and the artificially generated boundary layers are in equilibrium condition under the neutral state. All the other parameters are also very much within the expected trends.

The Monin-Obuckhov characteristic length can be calculated (Kaimal and Finnigan(1994)) according to

$$L = \frac{u_\tau^3 \overline{\theta_v}}{\varkappa g(q'/\rho c_p)}, \tag{28}$$

where $\overline{\theta_v}$ denotes the ambient temperature or the mean temperature above the boundary layer; $\varkappa$ is von Karman's constant and q' the heat flux at the wall. All other quantities take on their classical meaning.

The estimated value of q' was 314 W/m^2; then, it follows that for the naturally developed boundary layer L = -0.59 m, whereas for the artificially thickened boundary layer L = -0.60 m.

The Richardson number was evaluated according to:

$$R_i = \frac{g(T_H - T_B)(H - B)}{T(U_H - U_B)}, \tag{29}$$

where the subscripts H and B indicate the position in which the measurements are taken: H indicates the higher position of the probe, B indicates the lower position.

For neutral atmosphere the classical logarithmic wind profile is observed to occur. As the atmosphere becomes stable or unstable, the profile departs from its logarithmic shape so that appropriate corrections have to be applied.

Table 6: Richardson number for inner and outer layers.

	Stable	Neutral	Unstable
ABL	0.022	0	-0.021
Grainer and Meroney	0.004D	—	—
Ogawa et al.	—	—	-0.29
Layer 1, Artificial	0.001	0.0002	-0.037
Layer 1, Natural	0.001	0.0002	-0.036
Layer 2, Artificial	—	0	-0.005
Layer 2, Natural	0.001	0.0002	-0.036
Artificially thickened	0.004	0.0001	-0.027
Naturally thickened	0.022	0	-0.026

For the diabatic wind profile, the modified logarithmic profiles can be written as follows.

a) Stable flow.

$$u(z) = \frac{u_\tau}{\varkappa}\Big(\ln\frac{z}{z_0} + \gamma_m\frac{z}{L}\Big), \tag{30}$$

$$T(z) = T(z_0) + \alpha_h\frac{t_\tau}{\varkappa}\Big(\ln\frac{z}{z_0} + \gamma_h\frac{z}{L}\Big), \tag{31}$$

where u_τ is the friction velocity, z_0 is the roughness length, $\alpha_h = 0.74$ (Businger et al(1974)) or 1.0 (Dyer(1974)), t_τ is the friction temperature, $\gamma_h = 4.7$ (Businger et al(1974)) or 5.0 (Dyer(1974)).

b) Unstable flow.

$$u(z) = \frac{u_\tau}{\varkappa}\Big(\ln\frac{z}{z_0} - \psi_m\frac{z}{L}\Big), \tag{32}$$

$$T(z) = T(z_0) + \alpha_h\frac{t_\tau}{\varkappa}\Big(\ln\frac{z}{z_0} + \psi_h\frac{z}{L}\Big), \tag{33}$$

where

$$\psi_m = 2\ln\frac{1+x}{2} + \ln\frac{1+x^2}{2} - 2\tan^{-1}x + \frac{x}{2}, \tag{34}$$

with

$$x = (1 - \beta_m\frac{z}{L})^2 \tag{35}$$

and $\beta_m = 9$ (Businger et al.(1971)) or 16 (Dyer(1974)).

When the boundary layer is divided into two portions, an inner and an outer layer, the Richardson number can be evaluated using Eq.(29). Table 6 compares the results found at COPPE/UFRJ with the results of other wind tunnels and the atmospheric boundary layer.

Figure 6 shows the stream-wise variation of the temperature; it shows clearly that in the first two stations the temperature profiles have not yet accommodated to a logarithmic form. In fact, even the last two profiles cannot be considered in a equilibrium state. That is indication that for a quality profile the wind tunnel has to be further elongated.

The mean velocity profiles for naturally developed and artificially developed stable boundary layers are shown in Figures 7 and 8 in linear and logarithmic coordinates respectively. The temperature profile also in linear and logarithmic coordinates are shown in Figures 9 and 10 respectively. The Monin-Obukov length and the Richardson number are shown in Figures 11 and 12. The temperature stream-wise variation for the unstable case is shown in Figure 13. All these graphs are repeated for the unstable condition in Figures 14 through 19.

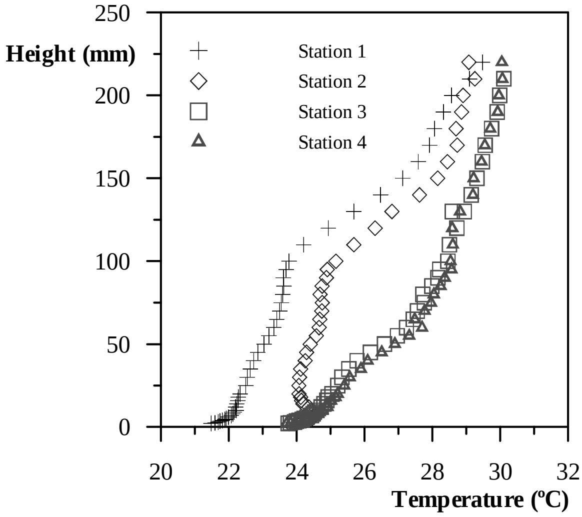

Figure 6. Temperature profiles in dimensional coordinates for several stream-wise stations; stable conditions.

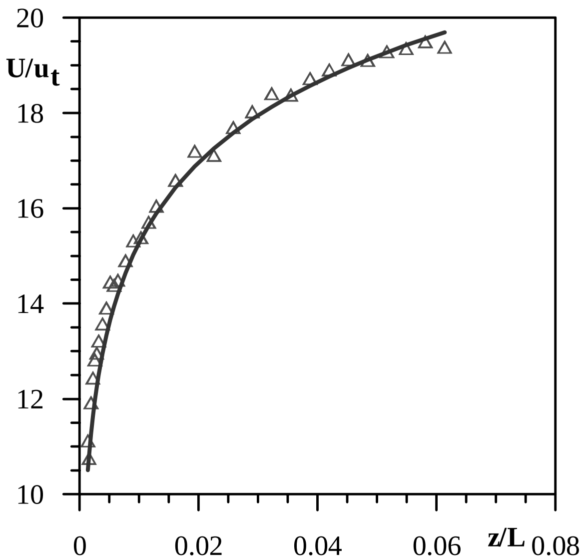

Figure 7. Velocity profiles in linear a scale; stable conditions.

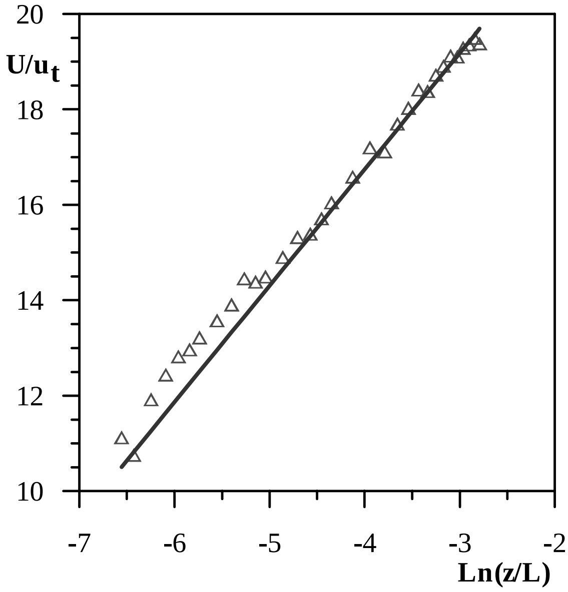

Figure 8. Velocity profiles in a logarithmic scale; stable conditions.

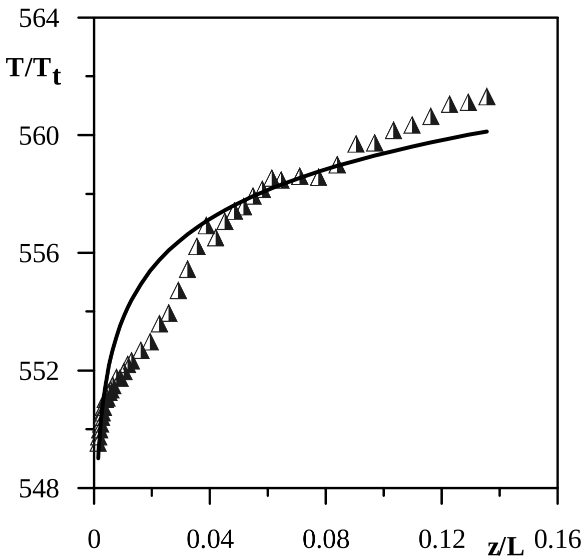

Figure 9. Temperature profiles in a linear and logarithmic scales; stable conditions.

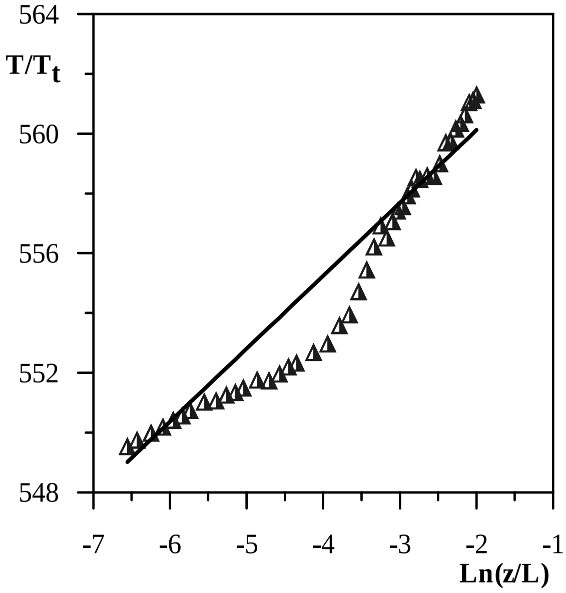

Figure 10. Temperature profiles in a logarithmic scale; stable conditions.

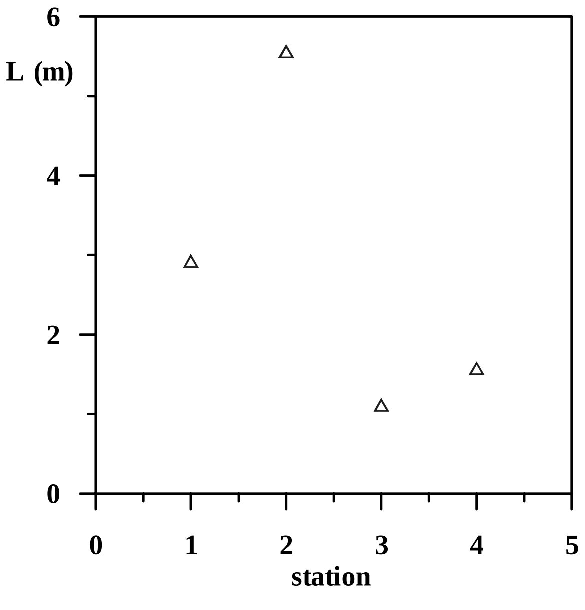

Figure 11. Monin-Obukov length; stable conditions.

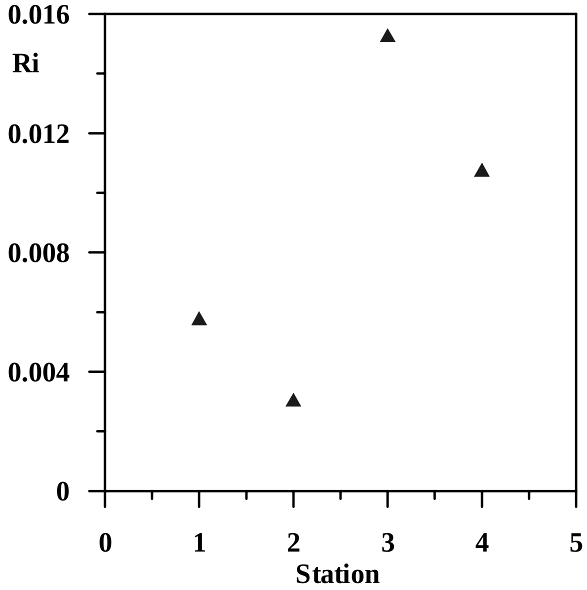

Figure 12. Richardson number; stable conditions.

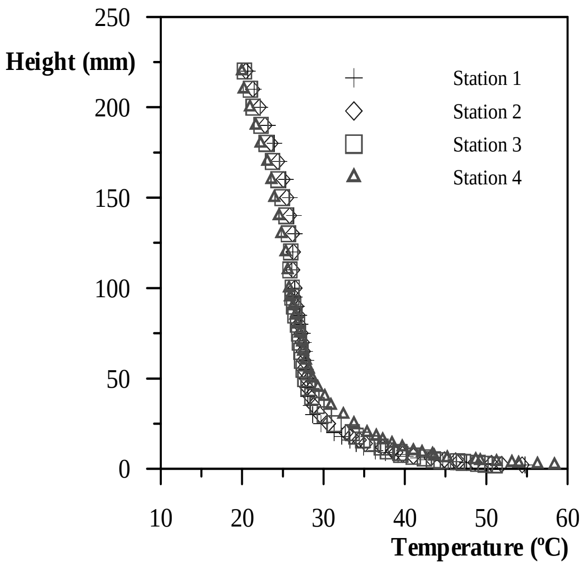

Figure 13. Temperature profiles in dimensional coordinates for several stream-wise stations; unstable conditions.

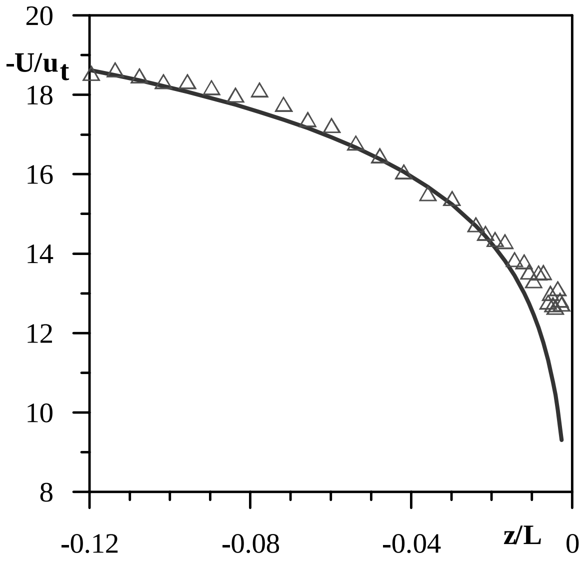

Figure 14. Velocity profiles in linear scale; unstable conditions.

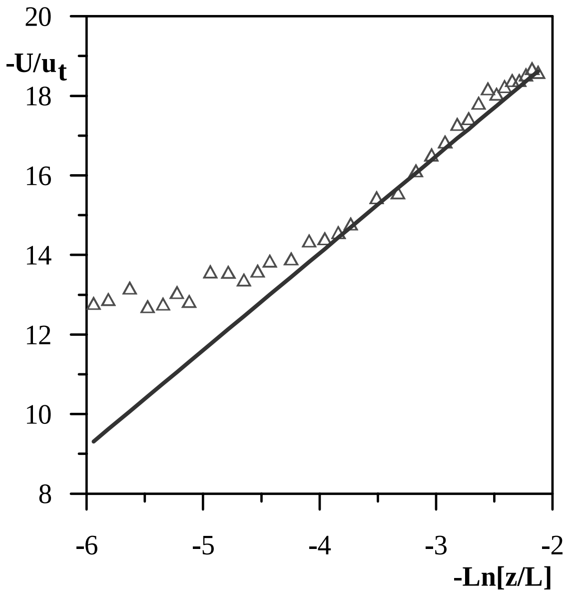

Figure 15. Velocity profiles in logarithmic scale; unstable conditions.

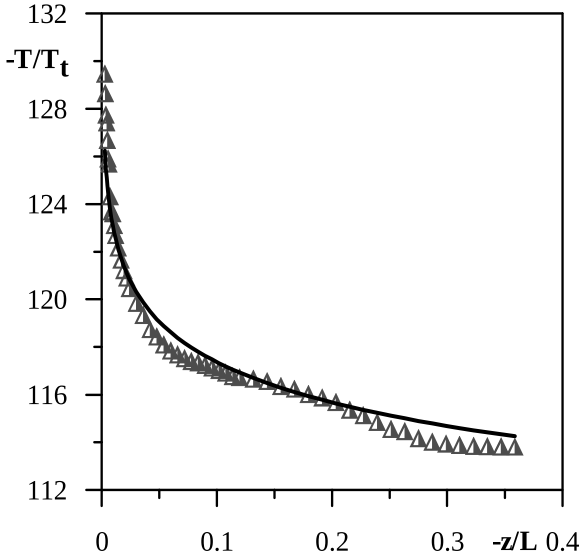

Figure 16. Temperature profiles in linear scale; unstable conditions.

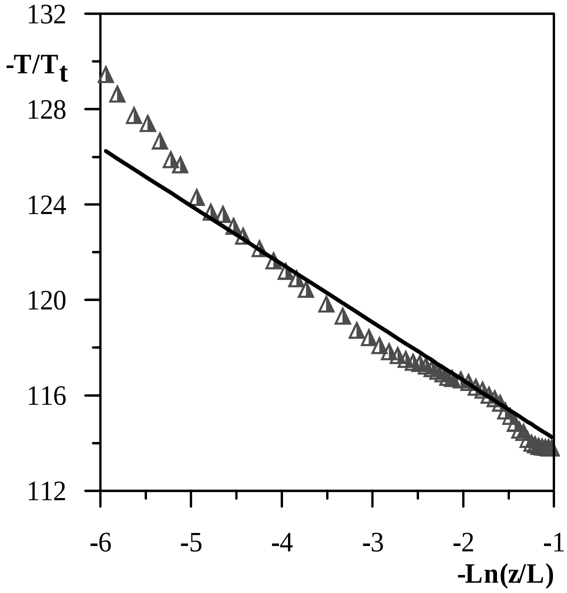

Figure 17. Temperature profiles in logarithmic scale; unstable conditions.

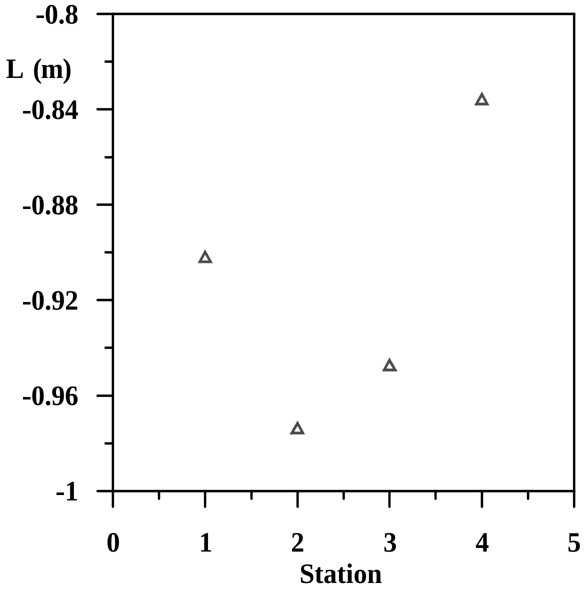

Figure 18. Monin-Obukov length; unstable conditions.

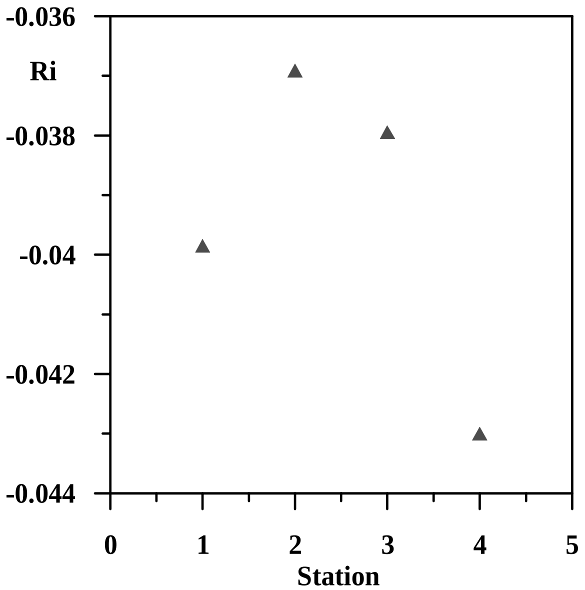

Figure 19. Richardson number; unstable conditions.

The results show that a good discrimination is obtained for all flow conditions. The logarithmic profile is strictly valid only for the neutral boundary layer. However, we have shown that for the stable and unstable flow conditions the departures from the logarithmic profile can be adequately represented by the Businger-Dyer relations. The skin-friction coefficient and the Stanton number have been estimated considering these relations valid.

The law of the wake has been reasonably well discriminated for all situations.

6. Conclusion

The present work has reported the recent progresses made at COPPE/UFRJ to construct a pilot wind tunnel which can generate boundary layers with characteristics close to those presented by an atmospheric flow. Results for stable, neutral and unstable flows were presented. In general, very satisfactory results were achieved. The velocity and temperature profiles were shown to adhere well to the atmospheric boundary layer features.

Acknowledgements. The present work was been financially supported by the CNPq through grant No 350183/93-7. MC and JBRL are also grateful to CNPq for the award of research scholarships.

7. References

Barbosa, P. H., Cataldi, M. and Silva Freire, A. P.; "Wind tunnel simulation of atmospheric boundary layer flows", 7th ENCIT, Porto Alegre, 2000.

Bremhorst, K., Effect of fluid temperature on hot-wire anemometers and an improved method of temperature compensation and linearisation without use of small signal sensitivities, J. Phys. E: Sci. Instr., 18, 44-49, 1985.

Businger, J.A., Wyngaard, J.C., Izuni, Y. and Bradley, E.F.; "Flux-profile relationships in the atmospheric surface layer", J. Atmos. Sci., Vol. 28, 181-189, 1971.

Cermak, J.E., "Laboratory Simulation of the Atmospheric Boundary Layer", AIAA J., Vol. 9, 1746-1753, 1971.

Cermak, J.E., "Application of Fluid Mechanics to Wind Engineering – A Freeman Scholar Lecture", J. Fluids Engng., Vol. 97, 9-38, 1975.

Cermak, J.E., "Wind Tunnel Design for Physical Modelling of Atmospheric Boundary Layers", Proceedings of ASCE, Vol. 107, 623-641, 1981.

Champagne, F. H., The temperature sensitivity of hot wires, Proc. Dynamic Flow Conf., Marseille, 101-113, 1978.

Dekeyeser, I. and Launder, B. E., A comparison of triple-moment temperature-velocity correlations in the asymmetric heated jet with alternative closure models, Proc. 4th Symp. on Turbulent Shear Flow, Univrsity of Karlsruhe, 14.1-14.8, 1983.

Dyer, A.J., "A Review of Flux-Profile Relationships", Bound.-Layer Meteor., Vol. 7, 363-372, 1974.

Fedorovich, E., Kaiser, R., Rau, M. and Plate, E.,"Wind Tunnel Study of Turbulent Flow Structure in the Convective Boundary Layer Capped by a Temperature Inversion", J. Atmosph. Sciences, Vol. 53, 1273-1289, 1996.

Fiedler, H., On data acquisition in heated turbulent flows, Proc. Dynamic Flow Conf., Marseille, 81-100, 1978.

Fulachier, L., Hot-wire measurements in low speed heated flows, Proc. Dynamic Flow Conf., Marseille, 465-487, 1978.

Freymuth, P., Hot-wire thermal calibration errors, Instr. and Contr. Systems, 43, 82-833, 1970.

Grainger, C. and Meroney, R., "Inverted Floor Wind-Tunnel Simulation of Stably Stratified Atmospheric Boundary Layer Flow", Atmosph. Envir., Vol. 28, 1887–1893, 1994.

Jerome, F. E., Guitton, D. E. and Patel, R. P., Experimental study of the wake interference between closely spaced wires of a X-type hot-wire probe, Aero. Quart., 22, 119-126.

Kaimal, J. C. e Finnigan, J. J.; Atmospheric boundary layer flow; Oxford University Press, 1994.

Koppius, A. M. and Trines, G. R. M., The dependence of hot-wire calibration on gas temperature at low Reynolds number, Int. J. Heat and Mass Transfer, 19, 967-974.

Lemieux, G. P. and Oosthuizen, P. H., A simple approach to the compensation of constant temperature hot-wire anemometers for fluid temperature fluctuations, Proc. 30th Int. Instrumentation Symp., Denver, AIAA, 277-282, 1984.

Meroney, R.N. and Melbourne, W.H., "Operating ranges of Meteorological Wind Tunnels for the simulation of Convective Boundary Layer(CBL) Phenomena", Boundary-Layer Meteor., Vol. 61, 145–174, 1992.

Ohba, R., Ukegushi, N., Kakishima, S e Lamb, B.; Wind tunnel experiment of gas diffusion in stably stratified flow over a complex terrain, Atmospheric Environment, 24A, 1987–2001, 1990.

Ogawa, Y., Diosey, P.G., Uehara, K. and Ueda, H., "A Wind Tunnel for Studying the Effects of Thermal Stratification in the Atmosphere", Atmosph. Envir., Vol. 15, 807–821, 1981.

Ohya, Y., Nakamura, Y. and Ozono, S.,“A Wind Tunnel for Studying Density-Stratified Flows”, Atmosph. Envir., Vol. 28, 1895–1900, 1994.

Pessoni, D. H. and Chao, B. T., A simple technique for turbulence measurements in nonisothermal air flows, Proc. 5th Int. Heat Transfer Conf., Tokyo, ISME, 278-282, 1974.

Poreh, M., Rau, M. and Plate, E.J., “Design Considerations for Wind Tunnel Simulations of Diffusion within the Convective Boundary Layer”, Atmosph. Envir., Vol. 25A, 1251–1256, 1991.

Rau, M., Bächlin, W. and Plate, E.J., “Detailed Design Features of a New Wind Tunnel for Studying the Effects of Thermal Stratification”, Atmosph. Envir., Vol. 25A, 1258–1263, 1991.